Reprinted from June 1988, Vol. 110, Journal of Mechanisms, Transmission, and Automation in Design

The Optimal Design of Squeeze Film Dampers for Flexible Rotor Systems

W. J. Chen*
M. Rajan
S. D. Rajan
H. D. Nelson
Mechanical and Aerospace Engineering,
Civil Engineering,
Arizona State University,
Tempe, Arizona 85287

Optimization techniques are employed to design squeeze film dampers for minimum transmitted load to the bearing and foundation in the operational speed range. The rotor systems are modeled by finite element formulation. The maximum transmitted load in the operational speed range is the objective function that is minimized using mathematical nonlinear programming (NLP) techniques. The damper design parameters are the radius, length, and radial clearance. Stability of the equilibrium solutions are investigated in the design procedure. Design derivatives have been determined in closed form expressions without resolution of the inherently nonlinear problem. A parametric study of the transmitted force is carried out to show the influence of damper parameters on the response and to demonstrate the merits of applying optimization techniques in damper design. Two numerical examples are presented that illustrate the effectiveness of optimizing squeeze film damper designs for reducing transmitted load.

Introduction

In high speed rotating machinery such as aircraft engines, generators, and compressors, the rotors may experience high vibrational amplitudes due to unbalance, thereby transmitting large forces to the bearings and the support structure. Modern high-speed gas turbine engines which require lightweight, hence, more flexible rotating assemblies make the design problem more difficult. It has been shown by several authors that appreciable attentuation of the unbalance displacement response and bearing forces can be obtained by using squeeze film dampers (SFD's) mounted in appropriately designed flexible supports (Lund, 1965; Gunter, 1966, 1970; Kirk and Gunter, 1972, 1973; Reiger, 1971). Recent publications (Mohan and Hahn, 1974; Cunningham et al., 1975; Gunter et al., 1977; Fleming, 1975; Rabinowitz and Hahn, 1983) have also presented the design methodology for sizing these nonlinear dampers. In particular there is a range of support damping and stiffness values which will improve rotor performance. Values outside this design range may result in substantially worse performance than that exhibited in the absence of SFD's (Mohan and Hahn, 1974; Cunningham et al., 1975; Barrett and Gunter, 1975).

However, the design of SFD's using automated optimization techniques has not been adequately addressed. The objective of the present study is to employ nonlinear programming techniques to design SFD's for minimum transmitted force to the bearing and foundation in the operational speed range. If the SFD is modelled using short bearing theory and the oil film is assumed to be fully cavitated, closed form expressions are obtained for the squeeze film nonlinear forces with the assumption of centered circular synchronous operation (Gunter et al., 1977; Taylor and Kumar, 1980). A solution technique developed by McLean and Hahn (1983) is used to determine the synchronous unbalance response of general large order systems incorporating SFD's. This procedure reduces the determination of unbalance response to a solution of a set of simultaneous nonlinear equations of order equal to the number of damper coordinates. The advantage of this technique is its ability to reduce the computation time and convergence difficulties. Once orbit eccentricities have been obtained, the unbalance response at other stations and the bearing forces can be easily determined. The design parameters used for a typical SFD are the damper radius, length, and radial clearance. The general consideration in the design of SFD's is to minimize the maximum transmitted load to the support structure in the operational spin speed range subject to constraints on the foregoing design variables as dictated by practical limitations. Stability of the equilibrium solutions can be investigated in the optimal design procedure to ensure stable operation. This involves the analysis of linearized perturbation equations about the equilibrium solutions. The design derivative (design sensitivity analysis) portion of any optimization algorithm constitutes a major segment of the total calculation. Thus, it is important to carry out the design sensitivity analysis as efficiently as possible. This is especially true for the design of nonlinear dampers in large order flexible rotor systems. The design sensitivities for SFD's are determined in closed form so it is not necessary to use finite differences to compute the sensitivity coefficients. The Min-Max design problem can be reduced to the parametric optimal design problem through introduction of an artificial design variable and a new constraint (Haug and Arora, 1979). The method of feasible directions (Vanderplaats, 1973; Rajan, S.

*Presently with Ingersoll-Rand Company, Mayfield, Kentucky.

Contributed by the Design Automation Committee for publication in the JOURNAL OF MECHANISMS, TRANSMISSION, AND AUTOMATION IN DESIGN. Manuscript received at ASME Headquarters, January 8, 1988.

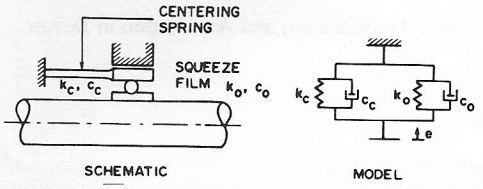

Fig. 1 Squeeze film damper

D., 1984) is employed for the solution of the design problem with only a penalty of an additional dimension in the design variable space.

Squeeze Film Damper Equations

A SFD is shown schematically in Fig. 1. It consists of a cylindrical journal, rolling element bearing, and a centering spring. It is assumed that the shaft precesses in a steady state circular concentric orbit about the fixed origin. The centering spring, shown in Fig. 1, can be considered as part of the SFD and is preloaded to offset any gravitational forces. The kinematic variables are defined as shown in Fig. 2. The geometric center of the displaced journal is located by polar coordinates (e,ϕ). Two unit vectors, $\hat{\mathbf{n}}_r$ and $\hat{\mathbf{n}}_t$, are oriented as shown parallel and perpendicular to the eccentricity vector, respectively. Two unit vectors, $\hat{\mathbf{n}}_Y$ and $\hat{\mathbf{n}}_Z$, serve as an inertial (fixed) reference frame. A third set of unit vectors, $\hat{\mathbf{n}}_y$ and $\hat{\mathbf{n}}_z$, define the (y,z) rotating reference frame. The centering spring is assumed to be isotropic and linear. The derivations of the nonlinear squeeze film forces are well documented in the literature (Barrett and Gunter, 1975). The resulting equations for the hydrodynamic forces in polar coordinates (r,t) are given by

$$\bar{\mathbf{F}}_r = \frac{-\mu RL^3}{C_r^3}\left\{\dot{\phi}e\left(\frac{2\epsilon}{(1-\epsilon^2)^2}\right)+\dot{e}\left(\frac{\pi(1+2\epsilon^2)}{2(1-\epsilon^2)^{5/2}}\right)\right\}\hat{\mathbf{n}}_r \tag{1}$$

$$\bar{\mathbf{F}}_t = \frac{-\mu RL^3}{C_r^3}\left\{\dot{\phi}e\left(\frac{2\pi}{2(1-\epsilon^2)^{3/2}}\right)+\dot{e}\left(\frac{\pi}{(1-\epsilon^2)^2}\right)\right\}\hat{\mathbf{n}}_t \tag{2}$$

Assuming circular synchronous motion, $\dot{\phi}=\Omega$ and e is constant, equations (1) and (2) become

$$\bar{\mathbf{F}}_r = \frac{-\mu RL^3}{C_r^3}\left\{\dot{\phi}e\left(\frac{2\epsilon}{(1-\epsilon^2)^2}\right)\right\}\hat{\mathbf{n}}_r \tag{3}$$

$$\bar{\mathbf{F}}_t = \frac{-\mu RL^3}{C_r^3}\left\{\dot{\phi}e\left(\frac{\pi}{2(1-\epsilon^2)^{3/2}}\right)\right\}\hat{\mathbf{n}}_t \tag{4}$$

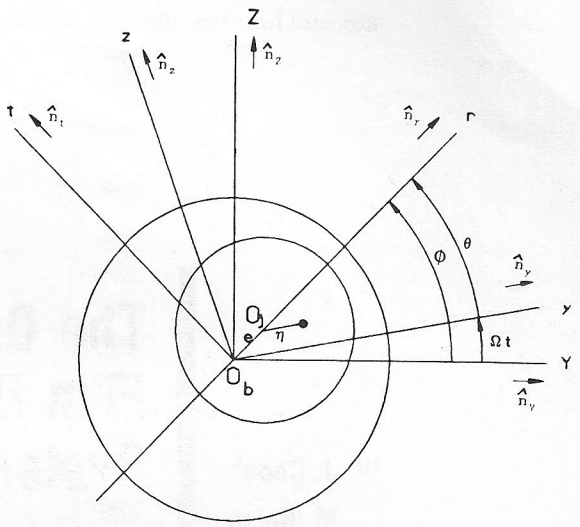

Fig. 2 Geometry and coordinate systems

The force in equation (3) appears as a stiffness coefficient times a displacement and it acts in a direction opposite to the bearing displacement. The equivalent bearing stiffness is:

$$K_0 = \frac{\mu RL^3}{C_r^3}\,\dot{\phi}\,\frac{2\epsilon}{(1-\epsilon^2)^2} \tag{5}$$

Since the bearing outer race is precessing and not rotating, every point in the journal has a velocity equal to $e\dot{\phi}$. The force in equation (4) therefore appears as a damping coefficient times a velocity and it acts in a direction opposite to the journal motion. The equivalent bearing damping is:

$$C_0 = \frac{\mu RL^3}{C_r^3}\,\frac{\pi}{2(1-\epsilon^2)^{3/2}} \tag{6}$$

These nonlinear forces in polar coordinates can be transformed to the fixed and rotating reference frame by the following coordinate transformations:

$$\begin{Bmatrix}\mathbf{F}_Y\\ \mathbf{F}_Z\end{Bmatrix} = \begin{bmatrix}\cos\phi & -\sin\phi\\ \sin\phi & \cos\phi\end{bmatrix}\begin{Bmatrix}\mathbf{F}_r\\ \mathbf{F}_t\end{Bmatrix} \tag{7}$$

for fixed frame coordinates, and

Nomenclature

a = weighting factor
$\bar{\mathbf{b}}$ = design variable vector $(NV\times 1)$
B = linearized damping coefficient defined by equation (31)
C = damping coefficient
$\underline{C}$ = damping factor
$\hat{C}$ = transformed damping matrix
$\bar{C}_r$ = squeeze film damper radial clearance
$\underline{D}_d$ = assembled damper dynamic stiffness matrix defined by equation (22)
e = displacement eccentricity $=(y^2+z^2)^{1/2}$
E = Young's modulus
$\mathbf{E}_d$ = nonlinear hydrodynamic force vector
f = objective function
$\mathbf{F}$ = force vector
g = inequality constraint
k = stiffness coefficient, linearized stiffness coefficient defined by equation (30)
$\underline{K}$ = stiffness matrix
$\bar{L}$ = damper length
$\underline{M}$ = mass matrix
$\hat{M}$ = transformed mass matrix
$\hat{\mathbf{n}}_r, \hat{\mathbf{n}}_t, \hat{\mathbf{n}}_y, \hat{\mathbf{n}}_z, \hat{\mathbf{n}}_y, \hat{\mathbf{n}}_z$ = unit vectors defined in Fig. 2
N = number of degrees of freedom
NV = number of design variables
ND = number of squeeze film dampers
NS = number of design support loads
$\bar{\mathbf{p}}$ = displacement vector (rotating frame)
$\mathbf{P}_r$ = reduced force vector defined by equation (19)

$$\begin{Bmatrix} \mathbf{F}_y \\ \mathbf{F}_z \end{Bmatrix} = \begin{bmatrix} \cos\theta & -\sin\theta \\ \sin\theta & \cos\theta \end{bmatrix} \begin{Bmatrix} \mathbf{F}_r \\ \mathbf{F}_t \end{Bmatrix} \tag{8}$$

for rotating frame coordinates

where $\cos\theta = \frac{y}{e}$, $\sin\theta = \frac{z}{e}$. (9), (10)

Note that $\phi = \theta + \Omega t$ is a function of time, hence, the forces expressed in the fixed frame are also functions of time.

By substitution of equations (3) and (4) using (5, 6, 9, 10), into equation (8), the time independent hydrodynamic forces in the rotating reference frame can be expressed as

$$\begin{Bmatrix} \mathbf{F}_y \\ \mathbf{F}_z \end{Bmatrix} = - \begin{bmatrix} K_0 & -\Omega C_0 \\ \Omega C_0 & K_0 \end{bmatrix} \begin{Bmatrix} y \\ z \end{Bmatrix}. \tag{11}$$

Steady State Solution

The use of finite elements for simulation of rotor systems has received considerable attention within the last few years. The works of Ruhl (1970) and Ruhl and Booker (1972) are the first examples of the studies using finite elements in rotor dynamics. Ruhl's finite element included translational inertia and bending stiffness but neglected rotatory inertia, gyroscopic moments, shear deformation, axial load, axial torque and internal damping. At about the same time Thorkildsen (1972) developed a finite element which was more general than Ruhl's in that it also included rotatory inertia and gyroscopic moments. Nelson and McVaugh (1976) used Rayleigh beam theory to develop a finite rotating shaft element which included the effects of translational and rotatory inertia, gyroscopic moments, and axial load. Later, Nelson (1980) added shear deformation to the Rayleigh beam theory to develop a Timoshenko beam element. In addition the element and system equations were developed in both a fixed and rotating reference frame. When analyzing systems with SFD's for steady state centered circular orbit response, it is convenient to use a rotating reference frame. The advantage of using such coordinates is that the time independent hydrodynamic forces can be determined by a relatively simple iterative procedure.

The assembled system equations of motion in both a fixed and rotating frame, details of which can be found in the paper by Nelson (1980) may be written as

$$\underline{M}\ddot{\bar{\mathbf{q}}} + \underline{C}\dot{\bar{\mathbf{q}}} + \underline{K}\bar{\mathbf{q}} = \bar{\mathbf{Q}}_{(N\times 1)} \tag{12}$$

for fixed reference coordinates, and

$$\underline{M}\ddot{\bar{\mathbf{p}}} + (\underline{C} + 2\Omega\underline{\hat{M}})\dot{\bar{\mathbf{p}}} + (\underline{K} - \Omega^2\underline{M} + \Omega\underline{\hat{C}})\bar{\mathbf{p}} = \bar{\mathbf{F}}_{(N\times 1)} \tag{13}$$

for rotating reference coordinates.

Note that $(\bar{\mathbf{q}}, \bar{\mathbf{p}})$ are the system displacement vectors in fixed and rotating reference frame, respectively, and $(\mathbf{Q}, \mathbf{F})$ are the vectors of the system unbalance excitation and hydrodynamic forces in fixed and rotating reference frame, respectively. If $\bar{\mathbf{p}}_0$ represents the steady state circular response of equation (13), then $\ddot{\bar{\mathbf{p}}}_0 = \dot{\bar{\mathbf{p}}}_0 = 0$, and equation (13) reduces to

$$(\underline{K} - \Omega^2\underline{M} + \Omega\underline{\hat{C}})\bar{\mathbf{p}}_0 = \bar{\mathbf{F}}_0 \tag{14}$$

For simplicity of notation, define

$$\underline{S} = (\underline{K} - \Omega^2\underline{M} + \Omega\underline{\hat{C}}) \tag{15}$$

as the system dynamical stiffness matrix.

For an N degree of freedom system, equation (14) consists of N nonlinear algebraic equations. A solution technique for determining the SFD eccentricities for flexible rotor systems such as defined by equation (14) is presented by Greenhill and Nelson (1981). Suffice it to say that as the number of simultaneous equations increases, the difficulties of convergence and of ensuring that all possible solutions have been found increase significantly. Recently, McLean and Hahn (1983) developed a solution technique for determining the synchronous unbalance response of general large order systems incorporating SFD's. Their procedure reduces the problem to solving a set of simultaneous nonlinear equations in the damper orbit eccentricities of an order equal to the number of damper coordinates. The technique is valid for all types of nonlinear supports where the radial and tangential forces are, for circular motions, functions of displacement and bearing parameters only. For a flexible rotor bearing system with multiple SFD's the procedure is presented below.

Partitioning equation (14) into a set of damper station coordinates, $\bar{\mathbf{p}}_d$ and its complement $\bar{\mathbf{p}}_c$, yields

$$\begin{bmatrix} \underline{S}_{cc} & \underline{S}_{cd} \\ \underline{S}_{dc} & \underline{S}_{dd} \end{bmatrix} \begin{Bmatrix} \bar{\mathbf{p}}_c \\ \bar{\mathbf{p}}_d \end{Bmatrix} = \begin{Bmatrix} \bar{\mathbf{F}}_c \\ \bar{\mathbf{F}}_d + \bar{\mathbf{E}}_d \end{Bmatrix} \tag{16}$$

where

$\begin{Bmatrix} \bar{\mathbf{F}}_c \\ \bar{\mathbf{F}}_d \end{Bmatrix}$ is the reordered system unbalance force vector $(N\times 1)$

Nomenclature (cont.)

$\bar{\mathbf{q}}$ = displacement vector (fixed frame)
$\mathbf{Q}$ = system unbalance excitation and hydrodynamic force vector (fixed frame)
R = damper radius
$\underline{S}$ = system dynamical stiffness matrix defined by equation (15)
$\underline{Sr}$ = reduced dynamical stiffness matrix defined by equation (20)
t = time
TR = transmitted force
(XYZ), (Xyz), (Xrt) = coordinates defined in Fig. 2
y, z = displacements
ϵ = damper eccentricity ratio $= e/C_r$
μ = squeeze film damper fluid viscosity
ρ = mass density
ϕ = angle between axes OY and Or
θ = angle between axes Oy and Or
Ω = spin speed
ψ = maximum transmitted load
η = disc mass eccentricity

Subscripts

c = centering, complementary set
d = squeeze film damper
i = index
k = iteration number
L = lower limit
o = circular orbit, steady state
r = radial, reduced
t = tangential
U = upper limit
y, z = displacement direction

and $\bar{\mathbf{E}}_d$ is the nonlinear hydrodynamic force vector ($2ND \times 1$). From the upper half of equation (16)

$$\bar{\mathbf{p}}_c = \underline{S}_{cc}^{-1}(\bar{\mathbf{F}}_c - \underline{S}_{cd}\bar{\mathbf{p}}_d) \tag{17}$$

which when substituted into the lower half yields

$$(\underline{S}_{dc}\underline{S}_{cc}^{-1}\bar{\mathbf{F}}_c - \bar{\mathbf{F}}_d) + (\underline{S}_{dd} - \underline{S}_{dc}\underline{S}_{cc}^{-1}\underline{S}_{cd})\bar{\mathbf{p}}_d = \bar{\mathbf{E}}_d. \tag{18}$$

For simplicity of notation, define

$$\bar{\mathbf{p}}_r = \underline{S}_{dc}\underline{S}_{cc}^{-1}\bar{\mathbf{F}}_c - \bar{\mathbf{F}}_d \tag{19}$$

$$\underline{S}_r = \underline{S}_{dd} = \underline{S}_{dc}\underline{S}_{cc}^{-1}\underline{S}_{cd} \tag{20}$$

Equation (18) can then be rewritten as

$$\bar{\mathbf{p}}_r + \underline{S}_r\bar{\mathbf{p}}_d = \bar{\mathbf{E}}_d(\bar{\mathbf{b}}, \bar{\mathbf{p}}_d) \tag{21}$$

Note that

$$\bar{\mathbf{E}}_d = -\underline{D}_d\bar{\mathbf{p}}_d \tag{22}$$

where $\underline{D}_d$ is an assembled dynamical stiffness matrix from equation (11) and the elements of $\underline{D}_d$ are functions of the eccentricity ratio and damper parameters.

The damper displacement vector $\mathbf{p}_d$ can then be obtained from

$$\bar{\mathbf{p}}_r + [\underline{S}_r + \underline{D}_d(\bar{\mathbf{b}}, \bar{\mathbf{p}}_d)]\bar{p}_d = \bar{0} \tag{23}$$

The damper displacement $\bar{\mathbf{p}}_d$ can be solved from the nonlinear equations (23) using some type of iterative solution scheme (Greenhill and Nelson, 1981; Hibner, 1975; IMSL) to determine the damper eccentricities and the associated equivalent stiffness and damping coefficients. Once the damper displacement vector $\bar{\mathbf{p}}_d$ has been found, the complementary displacement $\bar{\mathbf{p}}_c$ can be obtained directly from equation (17). From these displacements it is easy to calculate the element internal forces, moments and the forces transmitted through the bearings.

The magnitude of the transmitted load through a typical support station (Fig. 1) is given by

$$TR = (TR_y^2 + TR_z^2)^{1/2} \tag{24}$$

where

$$TR_y = (K_0 + K_c)y - \Omega(C_0 + C_c)z \tag{25}$$
$$TR_z = \Omega(C_0 + C_c)y + (K_0 + K_c)z$$

Stability and Sensitivity Analysis

The design of a rotor bearing system is an iterative process in which the parameters that influence the design performance are modified until the desired design objective is achieved. It should be noted that the variation of the squeeze film parameters can alter the location of peak responses and can also produce designs with multivalued responses. Whenever multiple solutions exist, all intermediate solutions are unstable and the high eccentricity responses usually produce large transmitted loads. Caution must, therefore, be used with this type of problem to be certain that the optimization procedure is applied in a range of values where the solution is in high orbit eccentricity and is also stable. The question as to which of the equilibrium solutions is stable or unstable (in the linear sense), can be investigated from the eigensolutions of the linearized perturbation equations as presented by McLean and Hahn (1984).

Design gradient (sensitivity) analysis plays an important role in modern structural optimization, since this allows the use of many of the more powerful gradient-based mathematical programming algorithms (Vanderplaats, 1982; Mangasarian, 1972). These derivatives are used in calculating the design change vector for each iteration. It may be noted that the design derivatives are also important in their own right. They represent trends that are important to the designer in changing the design estimate (Nelson et al. 1985). Thus, it is important to carry out the design sensitivity analysis as efficiently as possible if the algorithm is to be applied to large practical structures. Arora and Haug (1979) discussed a general procedure for calculation of design sensitivities that is employed in the current work. This work generalizes the previous works by considering the stability and sensitivity in the same model for the use of obtaining an optimal design.

If the steady state solution $\bar{\mathbf{p}}_0$ in equation (13) is perturbed by $\delta\bar{\mathbf{p}}$ to $\bar{\mathbf{p}}$, whereupon $\bar{\mathbf{F}}_0$ changes to $\bar{\mathbf{F}}(\bar{\mathbf{p}}, \dot{\bar{\mathbf{p}}}, \bar{\mathbf{b}})$, the first order perturbation equations of motion are given by

$$\underline{M}\delta\ddot{\bar{\mathbf{p}}} + \left(\underline{C} + 2\Omega\underline{\hat{M}} - \left[\frac{\partial\bar{\mathbf{F}}}{\partial\dot{\bar{\mathbf{p}}}}\right]_0\right)\delta\dot{\bar{\mathbf{p}}} + \left(\underline{K} - \Omega^2\underline{M} + \Omega\underline{\hat{C}} - \left[\frac{\partial\bar{\mathbf{F}}}{\partial\bar{\mathbf{p}}}\right]_0\right)\delta\bar{\mathbf{p}} = \left[\frac{\partial\bar{\mathbf{F}}}{\partial\bar{\mathbf{b}}}\right]_0\delta\bar{\mathbf{b}} \tag{26}$$

The derivatives in equation (26) are evaluated at the current design point $\bar{\mathbf{b}}_0$ and associated solution $\bar{\mathbf{p}}_0$. Note that the coefficients of $\delta\ddot{\bar{\mathbf{p}}}$, $\delta\dot{\bar{\mathbf{p}}}$ and $\delta\mathbf{p}$ in equation (26) are constants. The stability of the equilibrium solutions $\bar{\mathbf{p}}_0$ are established by the eigenvalues of the perturbed solutions $\delta\bar{\mathbf{p}}$ from the homogeneous form of equation (26). If any of the eigenvalues have nonnegative real parts, the solution is regarded as unstable in the linear sense.

The steady state unbalance response sensitivity can be determined by setting $\delta\ddot{\bar{\mathbf{p}}} = \delta\dot{\bar{\mathbf{p}}} = 0$ in equation (26). Since

$$\delta\bar{\mathbf{p}} = \nabla\bar{\mathbf{p}}^T\delta\bar{\mathbf{b}}, \tag{27}$$

the gradient of the unbalance response with respect to the design vector, evaluated at the current design point, can be determined by

$$\nabla\bar{\mathbf{p}}^T = \left(\underline{K} - \Omega^2\underline{M} + \Omega\underline{\hat{C}} - \left[\frac{\partial\bar{\mathbf{F}}}{\partial\bar{\mathbf{p}}}\right]_0\right)^{-1}\left[\frac{\partial\bar{\mathbf{F}}}{\partial\bar{\mathbf{b}}}\right]_0 \tag{28}$$

For a typical damper, the partial derivatives in equation (26) can be evaluated in the (r, t) coordinates and then transformed to the rotating references frame (y, z) by the coordinate transformation

$$\begin{Bmatrix}\Delta e \\ e_0\Delta\phi\end{Bmatrix} = \begin{bmatrix}\cos\theta_0 & \sin\theta_0 \\ -\sin\theta_0 & \cos\theta_0\end{bmatrix}\begin{Bmatrix}\Delta y \\ \Delta z\end{Bmatrix} \tag{29}$$

The transformation of the forces is given by equation (8) with $\mathbf{F}_r$ and $\mathbf{F}_t$ established by equations (1), (2). The perturbed linearized damper stiffness and damping matrices in (y,z) and (r,t) coordinates are related by:

$$\left[-\frac{\partial\bar{\mathbf{F}}}{\partial\bar{\mathbf{p}}}\right]_0 = \begin{bmatrix}K_{yy} & K_{yz} \\ K_{zy} & K_{zz}\end{bmatrix} = \begin{bmatrix}\cos\theta_0 & -\sin\theta_0 \\ \sin\theta_0 & \cos\theta_0\end{bmatrix}\begin{bmatrix}K_{rr} & K_{rt} \\ K_{tr} & K_{tt}\end{bmatrix}_0\begin{bmatrix}\cos\theta_0 & \sin\theta_0 \\ -sin\theta_0 & \cos\theta_0\end{bmatrix} \tag{30}$$

$$\left[-\frac{\partial\bar{\mathbf{F}}}{\partial\bar{\mathbf{p}}}\right]_0 = \begin{bmatrix}B_{yy} & B_{yz} \\ B_{zy} & B_{zz}\end{bmatrix} = \begin{bmatrix}\cos\theta_0 & -\sin\theta_0 \\ \sin\theta_0 & \cos\theta_0\end{bmatrix}\begin{bmatrix}B_{rr} & B_{rt} \\ B_{tr} & B_{tt}\end{bmatrix}_0\begin{bmatrix}\cos\theta_0 & \sin\theta_0 \\ -sin\theta_0 & \cos\theta_0\end{bmatrix} \tag{31}$$

where

$$\begin{bmatrix} K_{rr} & K_{rt} \\ K_{tr} & K_{tt} \end{bmatrix} = \frac{\mu R L^2}{C_r^3}\,\Omega \begin{bmatrix} \frac{4\epsilon_0(1+\epsilon_0^2)}{(1-\epsilon_0^2)^3} & \frac{-\pi}{2(1-\epsilon_0^2)^{3/2}} \\ \frac{\pi(1+2\epsilon_0^2)}{2(1-\epsilon_0^2)^{5/2}} & \frac{2\epsilon_0}{(1-\epsilon_0^2)^2} \end{bmatrix} \tag{32}$$

$$\begin{bmatrix} B_{rr} & B_{rt} \\ B_{tr} & B_{tt} \end{bmatrix} = \frac{\mu R L^3}{C_r^3} \begin{bmatrix} \frac{\pi(1+2\epsilon_0^2)}{2(1-\epsilon_0^2)^{5/2}} & \frac{2\epsilon_0}{(1-\epsilon_0^2)^2} \\ \frac{2\epsilon_0}{(1-\epsilon_0^2)^2} & \frac{\pi}{2(1-\epsilon_0^2)^{3/2}} \end{bmatrix} \tag{33}$$

In addition

$$\begin{bmatrix} \partial\bar{\mathbf{F}} \\ \partial\bar{\mathbf{b}} \end{bmatrix} = \begin{bmatrix} \cos\theta_0 & -\sin\theta_0 \\ \sin\theta_0 & \cos\theta_0 \end{bmatrix} \begin{bmatrix} \frac{\partial \mathbf{F}_r}{\partial R} & \frac{\partial \mathbf{F}_r}{\partial L} & \frac{\partial \mathbf{F}_r}{\partial C_r} \\ \frac{\partial \mathbf{F}_t}{\partial R} & \frac{\partial \mathbf{F}_t}{\partial L} & \frac{\partial \mathbf{F}_t}{\partial C_r} \end{bmatrix} \tag{34}$$

$$\begin{aligned}
\left(\frac{\partial \mathbf{F}_r}{\partial R}\right)_0 &= -\frac{\mu L^3}{C_r^3}\left\{\Omega e_0\left(\frac{2\epsilon_0}{(1-\epsilon_0^2)^2}\right)\right\} \\
\left(\frac{\partial \mathbf{F}_t}{\partial R}\right)_0 &= -\frac{\mu L^3}{C_r^3}\left\{\Omega e_0\left(\frac{\pi}{2(1-\epsilon_0^2)^{3/2}}\right)\right\} \\
\left(\frac{\partial \mathbf{F}_r}{\partial L}\right)_0 &= -\frac{3\mu R L^2}{C_r^3}\left\{\Omega e_0\left(\frac{2\epsilon_0}{(1-\epsilon_0^2)^2}\right)\right\} \\
\left(\frac{\partial \mathbf{F}_t}{\partial L}\right)_0 &= -\frac{3\mu R L^2}{C_r^3}\left\{\Omega e_0\left(\frac{\pi}{2(1-\epsilon_0^2)^{3/2}}\right)\right\} \\
\left(\frac{\partial \mathbf{F}_r}{\partial C_r}\right)_0 &= \frac{8\mu R L^3}{C_r^4}\left\{\Omega e_0\left(\frac{\epsilon_0}{(1-\epsilon_0^2)^3}\right)\right\} \\
\left(\frac{\partial \mathbf{F}_t}{\partial C_r}\right)_0 &= \frac{3\mu R L^3}{2C_r^4}\left\{\Omega e_0\left(\frac{\pi}{(1-\epsilon_0^2)^{5/2}}\right)\right\}
\end{aligned} \tag{35}$$

Optimal Design Procedure

Typically, design objectives for rotor systems include placement of critical speeds (Rajan, M., et al., 1987), minimization of response amplitudes and bearing loads, optimal choice of balance planes, and maximization of the onset of instability speed. In this work we restrict our attention to the minimization of transmitted load for steady unbalance with SFD's. The damper design parameters are the damper radius, length, and clearance. The maximum transmitted load to the supporting structure in the operational speed range is the objective function that is minimized and is subject to the bounds on the design variables. The design problem can be formulated as follows: Find the design vector $\bar{\mathbf{b}}$ to minimize

$$\psi = \underset{\Omega\epsilon[\Omega_L,\Omega_U]}{\text{Max}} \sum_i^{NS} a_i TR_i(\bar{\mathbf{b}}, \bar{\mathbf{p}}, \Omega) \tag{36}$$

subject to

$$\bar{\mathbf{b}}_L \le \bar{\mathbf{b}} \le \bar{\mathbf{b}}_U \tag{37}$$

the a_i represent weighting factors and Ω_L, Ω_U are the lower and upper bounds of the operating speed range.

The Min-Max design problem can be transformed to a standard nonlinear programming formulation by replacing the objective function by an artificial design variable b_{NV+1} and adding an additional contraint g. The design problem is then written in the standard format.

Minimize

$$f = b_{NV+1} \tag{38}$$

subject to the constraints

$$g = \frac{\psi}{b_{NV+1}} - 1 \le 0 \tag{39}$$

$$\bar{\mathbf{b}}_L \le \bar{\mathbf{b}} \le \bar{\mathbf{b}}_U \tag{40}$$

Any gradient-based nonlinear programming technique can iteratively locate a local minimum point to the problem by using the following four quantities (Rajan, S. D., 1984) at the kth design step:

(1) Value of objective function; $f = b_{NV+1}$.

(2) Value of constraint; $g = (\psi/b_{NV+1}) - 1$.

(3) Gradient of the objective function with respect to the design variables; $\nabla f_1 = \nabla f_2 = \ldots = \nabla f_{NV} = 0$; $\nabla f_{NV+1} = 1$.

(4) Gradient of the active constraints with respect to the design variables: $\nabla g_i = 1/b_{NV+1}\ (\partial\psi/\partial b_i)$, $i = 1, 2 \ldots NV$; $\nabla g_{NV+1} = -\psi/b_{NV+1}^2$

All these quantities can be obtained by the previous analyses. Using these function and gradient values, the solution technique computes the change in design to determine a new design point repetitively until the convergence criteria are satisfied. It is to be noted that the solution obtained may not be the global minimum. However, the chances of arriving at the global minimum can be increased by considering several sets of different starting values for the design parameters. At the optimum, the objective function value f is equal to the maximum transmitted load in the operational speed range ψ, i.e., the constraint g is active in optimum.

Numerical Examples

In order to demonstrate the automated design procedure, two numerical examples are presented. The first is taken from Gunter [9] and is a single mass centerd by preloaded springs. This simple system is instructive; however, the primary use of the design procedure is for large flexible rotor systems. Thus, a flexible system is also presented to illustrate the ability of the algorithm to deal with more complicated configurations.

Centered Single Mass System. The physical parameters of the system are summarized in Table 1.

The operational speed range considered is from 100 to 2000 R/s. For the baseline design, the maximum transmitted load occurs around 915 R/s and has a value of $TR = 1669.4$ N. Using the analytical procedure described earlier, a parametric study of the transmitted load is first carried out to understand the influence of the damper parameters on the transmitted load. Subsequently, the damper radius, length, and clearance are considered as design variables and the results are summarized in Table 2.

Table 1 Design data

m = 33.43 Kg	R = 64.8mm	R_L = 50.0mm	R_U = 70.0mm
η = 12.5μm	L = 22.7mm	L_L = 15.0mm	L_U = 35.0mm
K_c = 2.154x10^{7}N/m	C_r = 100μm	C_{r_L} = 50.0μm	C_{r_U} = 120.0μm
μ = 2.66x10^{-3}N·S/m^2			

Table 2 Optimal designs

Case	<design variable>	R(mm)	L(mm)	C_r(μm)	TR(N)	Ω(R/s)
0	baseline design	64.8	22.7	100.0	1669.4	915
1	C_r	64.8	22.7	<59.1>	888.6	1190
2	L	64.8	<35.0>	100.0	839.1	960
3	R	<70.0>	22.7	100.0	1616.2	915
4	C_r,L,R	<70.0>	<35.0>	<90.1>	724.9	1110

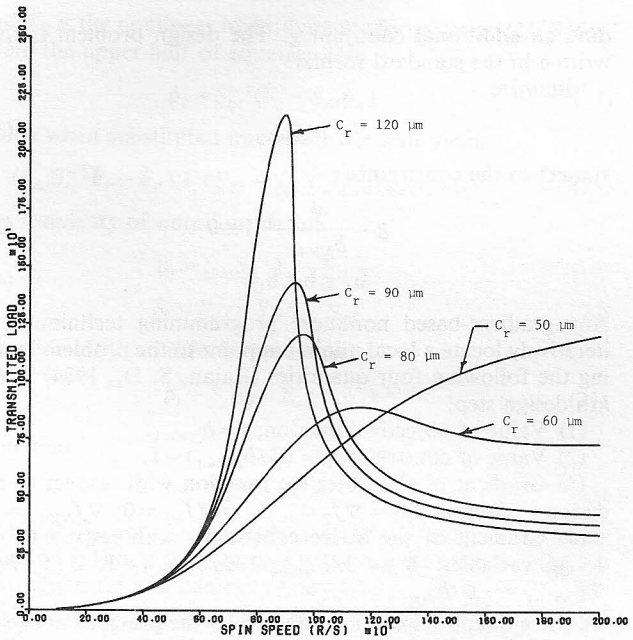

Fig. 3 Variation of transmitted load with damper radial clearance

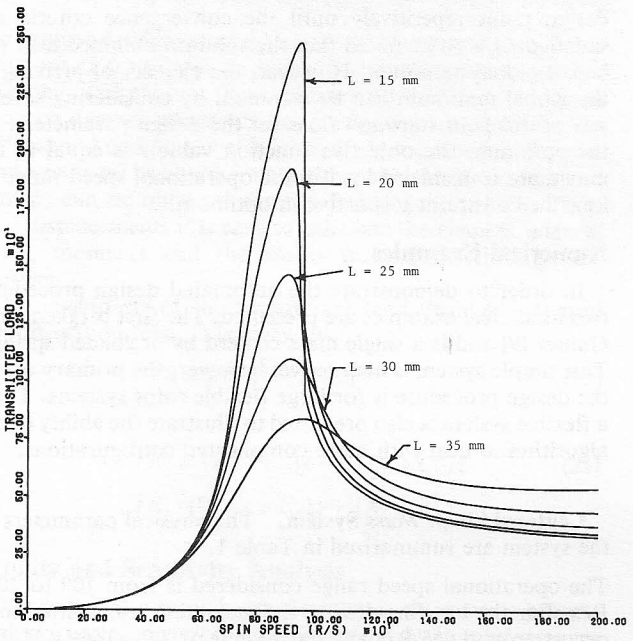

Fig. 4 Variation of transmitted load with damper length

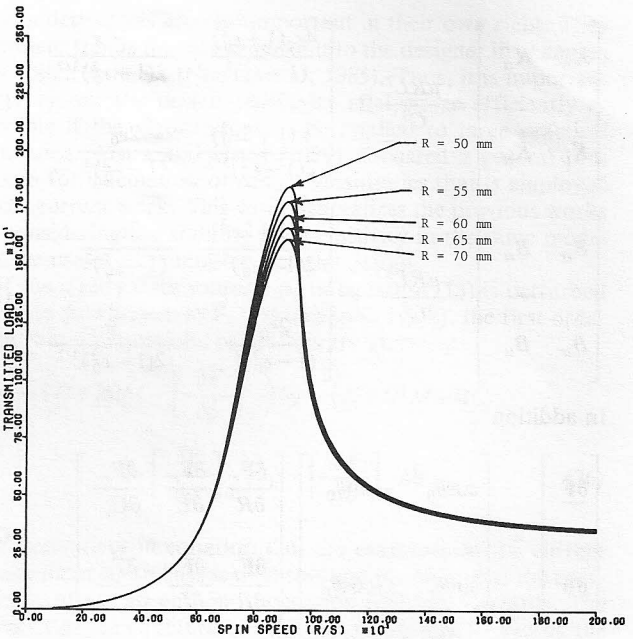

Fig. 5 Variation of transmitted load with damper radius

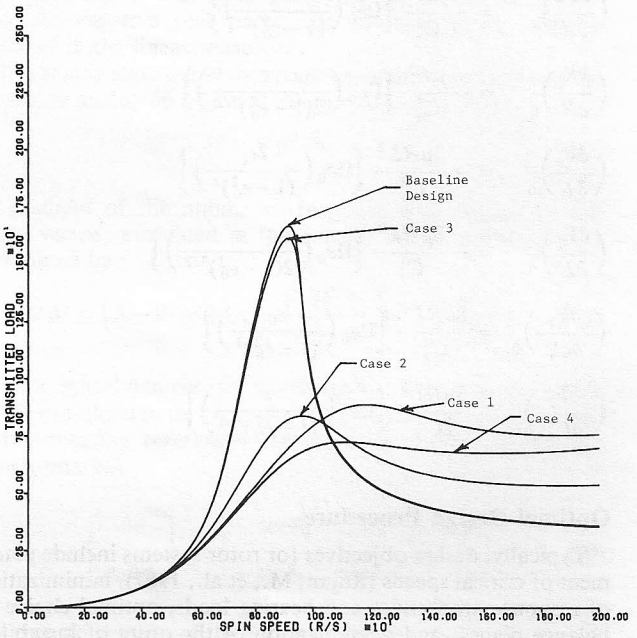

Fig. 6 Transmitted load for each design case

Case 1: The variation of the transmitted load versus spin speed with damper clearance as a parameter and all other variables held constant is shown in Fig. 3. For the lowest value of clearance shown, 50 μm, the journal does not possess a peak value in the operational speed range. However, the transmitted load gradually increases with speed to the upper limit of the operational speed range and has a value of $TR = 1202.8$ N. When the clearance is increased, however, peak values appear, and the maximum transmitted load occurs at different speeds for different damper clearance values. The optimal design is found to be $C_r = 59.1$ μm with a maximum transmitted force of $TR = 888.6$ N at 1190 R/s.

Case 2. Figure 4 shows the transmitted load versus spin speed with the damper length as a paraneter and all other variables held constant. It is shown that increasing the damper length monotonically lowers the maximum transmitted load. A jump phenomena can be observed for the lowest value, 15 mm, of damper length.

Case 3. In Fig. 5, the transmitted load is shown versus spin speed with damper radius as a parameter and all other variables held constant. The maximum transmitted load monotonically lowers as the damper radius increases.

Case 4: The damper clearance, radius and length are all considered to be design variables. The optimal design is determined to be $R = 70$ mm, $L = 35.0$ mm, $C_r = 90.1$ μm with a transmitted load of $TR = 724.9$ N at 1110 R/s. The maximum transmitted load corresponding to the optimum damper in case 4 is less than that corresponding to the optimal designs of the other three cases. This optimum design reduces the maximum transmitted load by 57 percent compared to that corresponding to the baseline design. The results of the optimization study are summarized in Table 2 and Fig. 6.

Table 3 Rotor configuration data

Element[1]	Length (cm)	Inner radius (cm)	Outer radius (cm)
1	4.27	1.42	2.95
2	4.62	1.42	2.95
3	1.60	1.42	2.95
4	9.68	1.42	2.95
5	7.46	1.96	2.95
6	16.51	2.69	2.95
7	15.24	2.69	2.95
8	15.24	2.69	2.95
9	15.24	2.69	2.95
10	15.24	2.26	2.95
11	14.93	1.42	2.95
12	7.92	2.31	2.95

[1] $E = 20.69 \times 10^6$ N/cm^2 $\rho = 8193$ kg/m^3

Table 4 Rotor concentrated disc data

Station No.	Mass (kg)	Polar Inertia (kg-cm^{2}x10^{-2})	Diametral Inertia (kg-cm^{2}x10^{-2})
1	11.38	19.53	9.82
4	7.88	16.70	8.35
5	7.70	17.61	8.80
12	21.71	44.48	22.24

Table 5 Rotor bearing data

Station No.	Stiffness (N/cm)	Damping (N-s/cm)
3	17,510	0
6	969,500	0
13	133,680	0

Table 6 Baseline and bounds on the damper parameters

R = 50.8mm	R_L = 44.45mm	R_U = 57.15mm
L = 25.4mm	L_L = 20.32mm	L_U = 30.48mm
C_r = 152.4μm	C_{r_L} = 76.20μm	C_{r_U} = 254.0μm

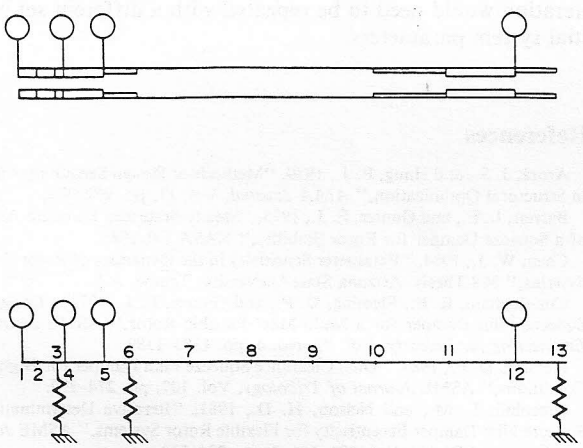

Fig. 7 Rotor schematic

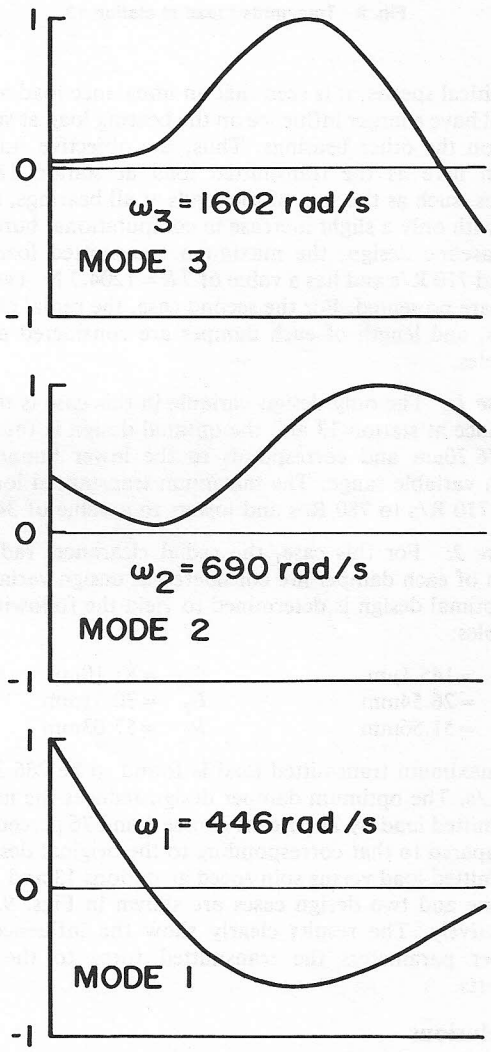

Fig. 8 Critical mode shapes

Flexible Rotor Example. A flexible rotor system is taken from Rajan, M., et al., (1987) as a second example. The rotor is modelled as a 13 station (12 element), 52 degree of freedom assembly with station locations as indicated in Fig. 7. Details of the rotor configurations and material properties are listed in Table 3. The rotor includes four rigid discs located at stations 1, 4, 5, and 12 with mass properties listed in Table 4. The rotor assembly is supported on a rigid foundation by isotropic undamped bearings with properties listed in Table 5. An SFD is included in parallel with the support stiffnesses at stations 3 and 13. The baseline and bounds on the design values for these two dampers are listed in Table 6.

The unbalance distribution for the rotating assembly consists of a cg eccentricity of 10.16μm for the concentrated disc at station 12. The first three undamped forward synchronous critical speeds are 383, 690, and 2300 R/s and the modes shapes are shown in Fig. 8. The operational spin speed range is selected to be 100 R/s to 2000 R/s which includes the first two critical speeds. By inspecting the mode shapes associated with

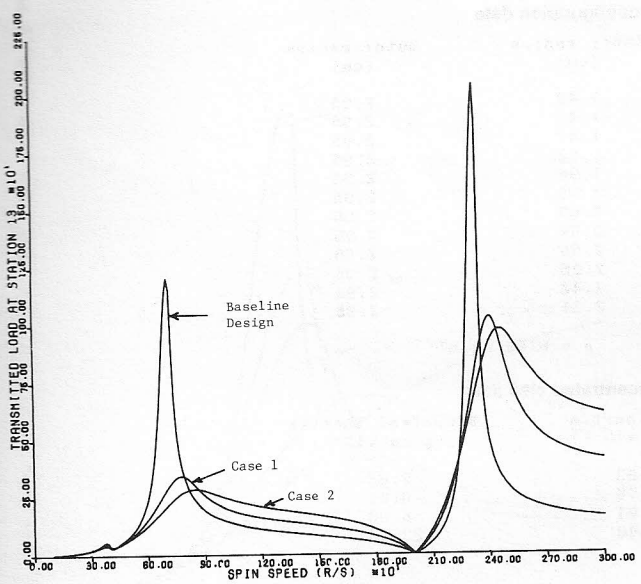

Fig. 9 Transmitted load at station 13

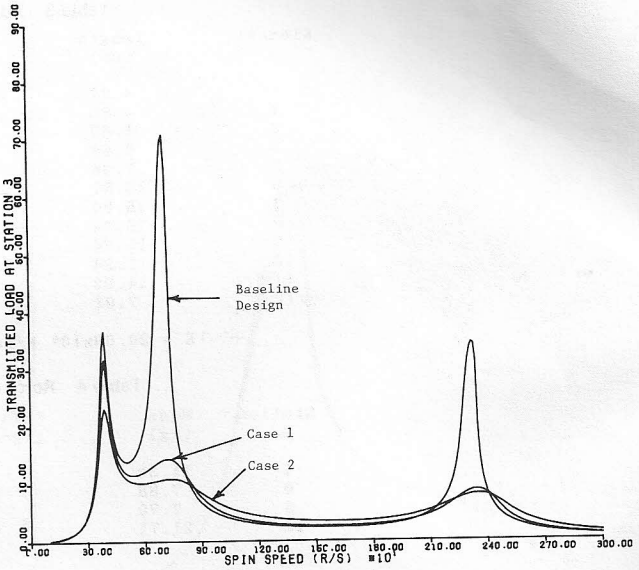

Fig. 10 Transmitted load at station 3

the critical speeds, it is seen that an unbalance load at station 12 will have a larger influence on the bearing load at station 13 than on the other bearings. Thus, the objective function is chosen here as the transmitted load at station 13. Other choices, such as the sum of the loads at all bearings, could be used with only a slight increase in computational burden. For the baseline design, the maximum transmitted load occurs around 710 R/s and has a value of $TR = 1204.7$ N. Two design cases are presented. For the second case, the radial clearance, radius, and length of each damper are considered as design variables.

Case 1: The only design variable in this case is the radial clearance at station 13 and the optimal design is found to be $C_r = 76.20\mu$m and corresponds to the lower bound of the design variable range. The maximum transmitted load shifts from 710 R/s to 780 R/s and lowers to a value of 344.9 N.

Case 2: For this case, the radial clearance, radius, and length of each damper are considered as design variables and the optimal design is determined to yield the following set of variables:

C_{r1}	$=145.1\mu$m	C_{r2}	$=81.10\mu$m
L_1	$=26.54$mm	L_2	$=30.31$mm
R_1	$=51.56$mm	R_2	$=57.03$mm

The maximum transmitted load is found to be 286.3 N near 850 R/s. The optimum damper design reduces the maximum transmitted load by 71 percent in case 1 and 76 percent in case 2 compared to that corresponding to the original design. The transmitted load versus spin speed at stations 13 and 3 for the baseline and two design cases are shown in Figs. 9 and 10, respectively. The results clearly show the influence of the damper parameters the transmitted force to the bearing supports.

Conclusions

The optimal design of squeeze film dampers to reduce the transmitted forces using optimization techniques has been presented. From the results of these investigations the following conclusions are drawn:

(*1*) The application of nonlinear programming techniques to the optimal design of squeeze film dampers in rotor-bearing systems can be achieved by setting up the problem as a min-max optimization problem.

(*2*) As the system is nonlinear it is capable of having multiple solutions for a given set of design variables. The problem of the optimal solution converging to an unstable solution is avoided by investigating the stability of the solution at intermediate design points during the optimal search and by limiting the design parameter set to high orbit eccentricities which normally correspond to stable solutions. If the search should tend to converge to an unstable solution the design iteration would need to be repeated with a different set of initial system parameters.

References

Arora, J. S., and Haug, E. J., 1979, "Methods of Design Sensitivity Analysis in Structural Optimization," *AIAA Journal*, Vol. 17, pp. 970–974.

Barrett, L. E., and Gunter, E. J., 1975, "Steady-State and Transient Analysis of a Squeeze Damper for Rotor Stability," NASA CR-2548.

Chen, W. J., 1984, "Parameter Sensitivity in the Dynamics of Rotor-Bearing Systems," MS Thesis, Arizona State University, Tempe, AZ.

Cunningham, R. E., Fleming, D .P., and Gunter, E. J., 1975, "Design of a Squeeze Film Damper for a Multi-Mass Flexible Rotor," ASME *Journal of Engineering for Industry*, Vol. 97, No. 4, pp. 1383–1389.

Fleming, D. P., 1985, "Dual Clearance Squeeze Film Damper for High Load Conditions," ASME *Journal of Tribology*, Vol. 107, pp. 274–279.

Greenhill, L. M., and Nelson, H. D., 1981, "Iterative Determination of Squeeze Film Damper Eccentricity for Flexible Rotor Systems," ASME *Journal of Mechanical Design*, Vol. 104, No. 2, pp. 334–338.

Gunter, E. J., 1966, "Dynamic Stability of Rotor-Bearing System," NASA SP-113, Washington.

Gunter, E. J., 1970, "Influence of Flexibility Mounted Rolling Element Bearings on Rotor Response Part 1—Linear Analysis," ASME *Journal of Lubrication Technology*, Vol. 92, No. 1, pp. 59–75.

Gunter, E. J., Barrett, L. E., and Allaire, P. E., 1977, "Design of Nonlinear Squeeze-Film Dampers for Aircraft Engines," ASME *Journal of Lubrication Technology*, Vol. 99, No. 1, pp. 57–64.

Haug, E. J., and Arora, J. S., 1979, *Applied Optimal Design*, Wiley Interscience, New York.

Hibner, D. H., 1975, "Dynamic Response of Viscous-Damped Multi-Shaft Jet Engines," *Journal of Aircraft*, Vol. 12, No. 4, pp. 305–312.

IMSL Library, International Mathematical and Statistical Libraries, Inc., Houston, Texas.

Kirk, R. G., and Gunter, E. J., 1972, "Effect of Support Flexibility and Damping on the Dynamic Response of a Single Mass Flexible Rotor in Elastic Bearings," NASA CR-2083.

Kirk, R. G., and Gunter, E. J., 1973, "Nonlinear Transient Analysis of Multimass Flexible Rotors—Theory and Application," NASA CR-2300.

Lund, J. W., 1965, "The Stability of an Elastic Rotor in Journal Bearings Wtih Flexible Damped Supports," ASME *Journal of Applied Mechanics*, Vol. 32, No. 4, pp. 911–920.

Mangasarian, O. L., 1972, "Techniques of Optimization," ASME *Journal of Engineering for Industry*, Vol. 94, pp. 365–372.

McLean, L. J., and Hahn, E. J., 1983, "Unbalance Behavior of Squeeze Film Damped Multi-mass Flexible Rotor Bearing Systems," ASME *Journal of Lubrication Technology*, Vol. 105, pp. 22–28.

McLean, L. J., and Hahn, E. J., 1984, "Squeeze-Film Dampers for Turbomachinery Stabilization," NASA CP-2338, pp. 391–405.

Mohan, S., and Hahn, E. J., 1974, "Design of Squeeze Film Damper Supports for Rigid Rotors," ASME *Journal of Engineering for Industry*, Vol. 96, No. 3, pp. 976–982.

Nelson, H. D., 1980, "A Finite Rotating Shaft Element Using Timoshenko Beam Theory," ASME *Journal of Mechanical Design*, Vol. 102, No. 4, pp. 783–804.

Nelson, H. D., and McVaugh, J. M., 1976, "The Dynamics of Rotor-Bearing Systems Using Finite Elements," ASME *Journal of Engineering for Industry*, Vol. 98, No. 2, pp. 593–600.

Nelson, H. D., Rajan, M., and Chen, W. J., 1985, "Sensitivity of Response Characteristics of Multi-Shaft Rotor Systems to Parameter Changes," NASA, NAG 3-580, Part VII.

Rabinowitz, M. D., and Hahn, E. J., 1983, "Optimal Design of Squeeze Film Supports for Flexible Rotors," ASME *Journal of Engineering for Power*, Vol. 105, pp. 487–494.

Rajan, M., Rajan, S. D., Nelson, H. D., and Chen, W. J., 1987, "Optimal Placement of Critical Speeds in Rotor-Bearing Systems," ASME *Journal of Vibration, Stress, and Reliability in Design*, Vol. 109, pp. 152–157.

Rajan, S. D., 1984, *OPTECH User's Manual*, Technical Report, Department of Civil Engineering, Arizona State University.

Reiger, N. F., 1971, "Unbalance Response of a Elastic Rotor in Damped Flexible Bearings at Supercritical Speeds," ASME *Journal of Engineering for Power*, Vol. 93, pp. 265–278.

Ruhl, R. L., 1970, "Dynamics of Distributed Parameter Rotor System: Transfer Matrix and Finite Element Techniques," Ph.D. dissertation, Cornell University.

Ruhl, R. L., and Booker, J. F., 1972, "A Finite Element Model for Distributed Parameter Turborotor Systems," ASME *Journal of Engineering for Industry*, pp. 128–132.

Taylor, D. L., and Kumar, B. R. K., 1980, "Nonlinear Response of Short Squeeze Film Dampers," ASME *Journal of Lubrication Technology*, Vol. 102, pp. 51–58.

Thorkildsen, T., 1972, "Solution of a Distributed Mass and Unbalanced Rotor System Using a Consistent Mass Matrix Approach," MSE Engineering Report, Arizona State University.

Vanderplaats, G. N., 1973, "Structural Optimization by Methods of Feasible Directions," *Computers and Structures*, Vol. 3, pp. 739–755.

Vanderplaats, G. N., 1982, "Structural Optimization—Past, Present, and Future," *AIAA Journal*, Vol. 20, No. 7, pp. 992–998.